Catena 163 (2018) 276–287

Contents lists available at ScienceDirect

Catena

journal homepage: www.elsevier.com/locate/catena

Empirical models of annual post-fire erosion on mulched and unmulched hillslopes

Sarah R. Schmeer[a], Stephanie K. Kampf[a,*], Lee H. MacDonald[b], Josh Hewitt[c], Codie Wilson[d]

[a] Department of Ecosystem Science and Sustainability, 1476 Campus Delivery, Colorado State University, Fort Collins, CO 80523-1476, United States
[b] Natural Resource Ecology Laboratory, 1499 Campus Delivery, Colorado State University, Fort Collins, CO 80523-1499, United States
[c] Department of Statistics, 1877 Campus Delivery, Colorado State University, Fort Collins, CO 80523-1877, United States
[d] Department of Geosciences, 1482 Campus Delivery, Colorado State University, Fort Collins, CO 80523-1482, United States

ARTICLE INFO

Keywords:
Hillslope erosion
High Park Fire
Wildfire
Bare soil
Erosion modeling
Mulch

ABSTRACT

Erosion is one of the primary land management concerns following wildfire. This study examines controls on post-fire hillslope-scale erosion for the 2012 High Park Fire in northern Colorado, develops simple empirical models for predicting post-fire sediment yields, and evaluates model performance on several nearby fires. From 2013 to 2015 we collected ground cover, rainfall, topographic, and sediment yield measurements from 29 convergent hillslopes; eight of these hillslopes had varying amounts of mulch applied to reduce erosion. From these data we examined correlations between annual sediment yield and three categories of predictor variables (ground cover, precipitation, and topography). Percent bare soil was the single largest control on sediment yield, followed by rainfall variables. Sediment yield generally decreased with flow path length, but the correlation was weak. The empirical models each predicted sediment yield with three variables: percent bare soil, one precipitation variable, and one topographic variable. The models had similar accuracy for the High Park Fire using varying combinations of precipitation and topographic variables (Nash-Sutcliffe coefficients 0.70–0.84). An empirical model predicting annual sediment yields as a function of percent bare soil, June–October precipitation, and the maximum flow path length had variable performance when applied to other fires in the same region, with predictions ranging from poor to good for individual fires and Nash-Sutcliffe coefficients of 0.26–0.32 for all fires combined. These tests show some promise for applying the empirical model to fires in the study region, but further model testing is needed to determine the range of conditions under which the model can be applied.

1. Introduction

Wildfires are increasing in frequency, extent, and severity in many regions throughout the world (Flannigan et al., 2009; Miller et al., 2009; Dennison et al., 2014). Elevated erosion after wildfire can impact downstream water quality, fill reservoirs, and damage aquatic habitat (Shakesby and Doerr, 2006; Goode et al., 2012), so land managers need to predict reliably which areas on the landscape have high post-fire erosion risk. Empirical regression models have been developed to predict post-fire erosion rates at individual research sites (Benavides-Solorio and MacDonald, 2005; Pietraszek, 2006), but these often use the particular variables collected in the study area and are not easily transferred to other fires. Process-based hillslope erosion models such as RUSLE (Renard et al., 1997), Disturbed WEPP (Elliott, 2004), and ERMiT (Robichaud et al., 2007) have shown variable performance for predicting annual post-fire erosion rates on individual hillslopes (Larsen and MacDonald, 2007; Fernández et al., 2010; Robichaud et al., 2016), so there is still a role for ongoing research on post-fire erosion prediction, particularly given the wide range of post-fire conditions.

Post-fire emergency response teams around the world have developed excellent tools for determining what parts of the landscape are most vulnerable to erosion after fire (Robichaud et al., 2007; Goodrich et al., 2005; Vafeidis et al., 2007; Van Eck et al., 2016), yet sediment yield remains one of the most difficult physical variables to predict accurately. Inaccuracies in sediment yield predictions can relate to the quality of input and sediment yield data, scale of application, and adequacy of model structure. Hillslope erosion models generally require inputs related to ground cover, soil erodibility, precipitation, and topography (Woolhiser et al., 1990; Renard et al., 1997; Elliott, 2004). Research projects on post-fire erosion have collected ground cover information through field surveys and derived soil properties from field samples (Benavides-Solorio and MacDonald, 2005; Pietraszek, 2006),

* Corresponding author.
E-mail addresses: sarah.schmeer@colostate.edu (S.R. Schmeer), stephanie.kampf@colostate.edu (S.K. Kampf), lee.macdonald@colostate.edu (L.H. MacDonald), joshua.hewitt@colostate.edu (J. Hewitt), codie.wilson@colostate.edu (C. Wilson).

https://doi.org/10.1016/j.catena.2017.12.029
Received 9 February 2017; Received in revised form 20 December 2017; Accepted 22 December 2017

but it is infeasible to collect such field data over entire watersheds. Soil properties are particularly difficult to represent accurately because they are heterogeneous across hillslopes (Russo et al., 1997), change as a result of burning and burn severity (Larsen and MacDonald, 2007), and can change over time due to surface armoring (e.g., Morris and Moses, 1987; Schaffrath, 2009). Where detailed field measurements of ground cover and soils are lacking, post-fire erosion model applications derive ground cover from land cover and burn severity maps and soil properties from soil survey maps (Vafeidis et al., 2007; Terranova et al., 2009). Some erosion model applications have developed look-up tables that use pre-fire land cover and burn severity to predict ground cover and changes in soil properties (Elliott, 2004; Canfield and Goodrich, 2005).

Rainfall intensity is a key control on hillslope erosion after burning (Spigel and Robichaud, 2007; Kampf et al., 2016), but many areas lack the fine resolution rainfall data needed to capture spatial and temporal storm patterns. Post-fire erosion models therefore use a variety of estimation strategies for quantifying the precipitation input. For example, applications of the Revised Universal Soil Loss Equation (RUSLE) typically use mean annual rainfall erosivity, which combines the kinetic energy of total rainfall with maximum storm intensity (Brown and Foster, 1987). The Water Erosion Prediction Project (WEPP) model generally uses stochastic rainfall intensity characteristics generated from daily long-term precipitation data (Flanagan and Livingston, 1995), or it can directly use rain gauge data. Similarly, the KINEROS2 erosion model uses rainfall hyetographs from either rain gauge measurements or design storms (Woolhiser et al., 1990).

Topographic variables such as hillslope length and slope may be the easiest to obtain after fires because of the widespread availability of digital elevation data, although these variables are affected by the scale of topographic data (Thompson et al., 2001). Commonly applied hillslope erosion models such as RUSLE and WEPP were developed and calibrated to data collected primarily from relatively small plots. The standard plots used to develop the Universal Soil Loss Equation were 22 m long (Renard et al., 2011), and many of the plots used to develop WEPP were 9–11 m long (Laflen et al., 1991). For post-fire applications hillslope erosion assessments are usually needed over much larger areas for which field measurements of erosion are more difficult to obtain.

The goal of this research is to develop and test simple empirical hillslope-scale erosion prediction models that use commonly measured post-fire variables. We develop the models based on field data collected in the area burned by the 2012 High Park Fire in north-central Colorado and test them using field data from five other fires in the region. Our specific objectives are to: (1) quantify post fire ground cover, rainfall, and annual sediment yields for unmulched and mulched hillslopes; (2) examine how ground cover, rainfall, and topographic variables relate to annual hillslope sediment yields; (3) develop empirical models to predict annual hillslope-scale sediment yields; and (4) test the performance of these models against measured sediment yields from other fires in the Colorado Front Range.

2. Study site

The High Park Fire burned in June 2012, and its perimeter encompassed about 350 km^2 of mostly forested land west of Fort Collins, Colorado (BAER, 2012) (Fig. 1). Our study sites were located within two ~15 km^2 watersheds, Skin Gulch and Hill Gulch, that each had about 65–70% of their area burned at high or moderate severity. These watersheds were selected because they have similar size, aspect and burn severity, and both drain directly to the Cache la Poudre River. Hill Gulch is the eastern watershed with elevations ranging from 1740 to 2380 m, and Skin Gulch is slightly larger and higher with an elevation range of 1890 to 2580 m. Prior to burning the vegetation at lower elevations was primarily ponderosa pine (*Pinus ponderosa*) with grasses and shrubs in drier south-facing and lower elevation areas. Higher elevations in the burned area had a denser mixed conifer forest (BAER, 2012). The primary soil within the watersheds is Redfeather sandy loam (BAER, 2012), and this is a shallow to moderately deep (40–100 cm), well-drained sandy loam formed on granitic bedrock; the taxonomic description is loamy-skeletal, mixed, superactive Lithic Glossocryalfs (Moreland, 1980; USDA NRCS, 1998). Soils are often shallow and rocky, with rock outcrops on many of the steeper hillslopes and ridgetops.

Average annual precipitation in the burned area ranges from approximately 440 to 600 mm (PRISM Climate Group), and precipitation falls as snow during the winter months. Summer rain events are typically spatially variable, high-intensity convective storms. The area also experiences occasional low-intensity frontal storms, particularly in the spring and fall (MacDonald and Stednick, 2003). Previous studies have shown that nearly all of the post-fire erosion in this region results from higher-intensity summer thunderstorms rather than snowmelt or lower intensity frontal storms (Benavides-Solorio and MacDonald, 2005; Wagenbrenner et al., 2015).

3. Methods

3.1. Field methods

After the fire we installed 29 sediment fences (similar to Robichaud and Brown, 2002) to capture post-fire erosion from convergent hillslopes. Fences were installed in areas with moderate to high burn severity in the central axes of convergent hillslopes. Locations were selected to represent a range of slope lengths, slope angles and contributing areas. Contributing areas to the fences were delineated in the field using a Juno Trimble handheld GPS with horizontal accuracy of < 5 m. These field delineations gave hillslope contributing areas ranging from 0.1–1.5 ha (Table 1). For nine hillslopes with particularly large contributing areas or long slope lengths, we installed two fences in succession to increase sediment storage capacity. We established twenty-one of the sediment fences in August–September 2012 and eight in May–June 2013. The measured hillslopes were in five clusters of 4–7 sites at different elevations of each of the study watersheds (Fig. 1; Table 1). Each hillslope ID begins with the name of the watershed (S for Skin Gulch; H for Hill Gulch) followed by the elevation zone (L for lower; M for middle; U for upper) and the hillslope number (Fig. 2; Table 1).

Each hillslope cluster was co-located with one or more Rainwise tipping bucket rain gauges with a 0.25 mm resolution and data loggers to record the time of each tip. Sediment fences were located 10–830 m away from the nearest rain gauge. To the extent possible, we checked fences for sediment after each rain storm and at the beginning (late October) and end (late April) of the winter snowmelt season from 2013 to 2015. During each site visit we manually removed trapped sediment and measured the field mass to the nearest 0.5 kg on a hanging scale. For each sediment measurement we collected a representative soil sample, dried it in the lab to determine the water content, and used the water content to convert the wet sediment mass to a dry mass. We estimate that the soil samples contained < 1% organic matter, although another study on severely burned slopes in a more humid climate measured 5–7% organic matter (Robichaud et al., 2006). The dry mass was divided by the contributing area to obtain sediment yield (*SY*) in $Mg\ ha^{-1}$.

Management agencies applied wood shred mulch at a planned rate of 6 $Mg\ ha^{-1}$ to four of the studied hillslopes (HU1–4) in November 2012 (Fig. 2b) and straw mulch in June 2013 at a planned rate of 3–4 $Mg\ ha^{-1}$. The wood shreds had stubble lengths of 10–20 cm, < 3 cm diameter, and minimal fines (NRCS, 2013). Straw mulch was applied to two of the hillslopes that had wood shred mulch (HU3,4) and four additional hillslopes (HL5,6; SU1,2). Of the latter four sites, straw coverage was sparse and clumpy on HL5 and HL6 and dense and evenly distributed on SU1 and SU2 (Fig. 2a). Four hillslopes in HL (HL1–4) also had scattered mulch cover (≤ 5%) in June 2013 that had blown in from

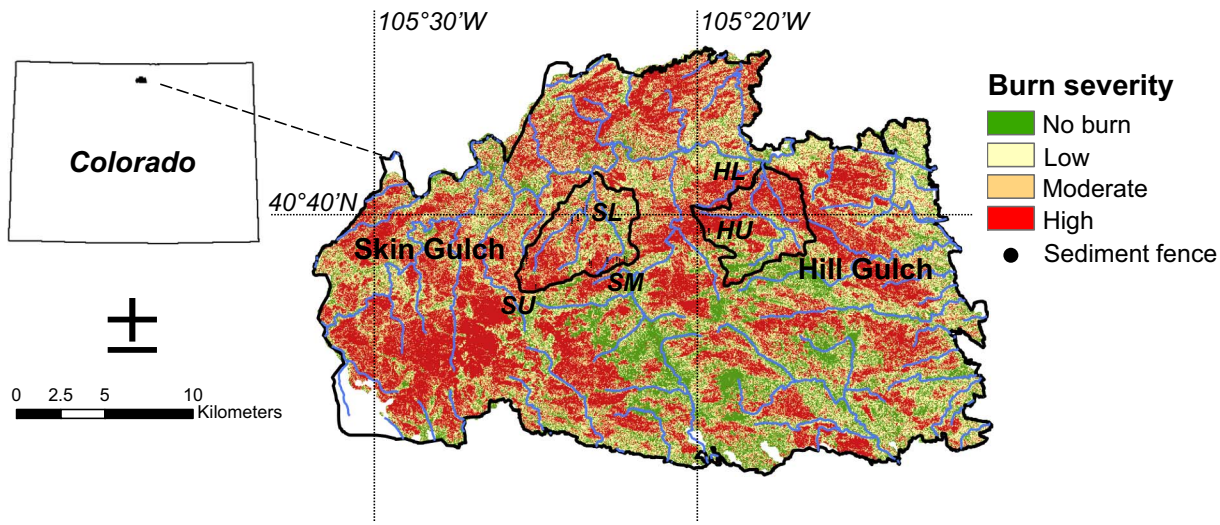

Fig. 1. Locations of hillslope sediment fences and the watershed boundaries of Skin Gulch and Hill Gulch overlain on a burn severity map of the High Park Fire. Clusters of sediment fences are labeled by watershed (S = Skin; H = Hill) and elevation zone (L = lower; M = middle; U = upper). Burn severity map from Stone (2015).

nearby mulched areas. Mulch applications were not part of our initial study design, but they presented the opportunity to examine the influence of mulch on hillslope sediment yields.

We measured percent surface cover in each hillslope area by systematic point counts along transects at the end of the 2012 growing season and at the beginning and end of the 2013–2015 growing seasons. Each survey had a minimum of 100 points, and each point was classified as bare soil, live vegetation, litter, rock larger than 1 cm in diameter, wood larger than 1 cm in diameter, tree, straw mulch, or wood shred mulch.

3.2. Data analysis and model development

Our data analysis and modeling covers summer 2013 to fall 2015. Throughout this manuscript, year 0 is the year of the fire; year 1 is the year after the fire, and so on. We excluded 2012 (year 0) from the analysis because not all fences and mulch were in place, and we missed nearly all of the larger storms that caused erosion and channel aggradation in that year (Brogan et al., 2017). We divided the hillslopes into three subsets: unmulched (HLD1; all SL and SM; SU3–6; n = 17), sparsely mulched (HL1–4), and mulched (HL5–6; HU1–4; SU1–2; n = 8). We compared ground cover changes and erosion rates over time

Table 1
Hillslope IDs, contributing area characteristics, and total sediment yield (*SY*) from 2013 to 2015. Mulch type is either agricultural straw ("straw") or wood shreds ("wood"). For sites with sparse (≤ 5% mulch), the mulch type is in italics. *SY*s for the five highest erosion sites are highlighted in bold.

Hillslope	Area (ha)	Longest flow path length (m)	Mean slope (m/m)	Max topo index	June 2013% mulch cover	Mulch type	*SY* (Mg ha^{-1})		
							2013	2014	2015
HL1	0.08	48	0.29	1.35	5	*Straw*	**22.8**	**3.4**	**0.4**
HL2	0.10	69	0.33	0.82	4	*Straw*	**38.2**	**1.1**	**0.1**
HL3	0.18	99	0.41	1.15	2	*Straw*	8.6	0.1	0.0
HL4	0.09	80	0.42	0.77	1	*Straw*	**23.7**	**2.9**	**0.2**
HL5	0.15	65	0.33	0.40	20	Straw	9.0	0.6	0.8
HL6	0.21	79	0.38	1.88	29	Straw	4.8	0.4	1.6
HLD1	0.23	134	0.56	2.13	0		17.1	0.1	0.0
HU1	0.19	102	0.39	1.64	65	Wood	0.6	0.0	0.0
HU2	0.26	89	0.29	1.79	44	Wood	2.3	0.1	0.0
HU3	0.32	151	0.34	2.30	20	Straw + Wood	4.7	1.3	1.1
HU4	0.19	77	0.34	1.39	35	Straw + Wood	3.1	0.2	0.0
SL1	0.45	223	0.53	3.07	0		11.4	0.1	0.0
SL2	0.36	171	0.63	2.53	0		7.4	0.0	0.0
SL3	0.83	218	0.55	3.59	0		5.5	0.0	0.0
SL4	0.25	147	0.49	1.33	0		11.7	0.1	0.0
SL5	0.34	134	0.43	1.98	0		11.6	0.0	0.0
SLD1	1.31	266	0.55	4.53	0		6.1	0.0	0.0
SM1	0.16	110	0.37	2.60	0		13.7	0.3	0.0
SM2	0.25	139	0.37	1.69	0		12.6	1.0	0.0
SM3	0.34	157	0.34	2.73	0		13.1	1.4	0.0
SM4	0.13	82	0.21	1.70	0		15.3	0.1	0.0
SM5	0.19	90	0.52	1.13	0		**25.3**	**3.7**	**0.0**
SM6	0.09	75	0.42	0.58	0		**37.6**	**6.8**	**0.1**
SU1	0.44	158	0.27	2.21	51	Straw	0.1	0.0	0.0
SU2	0.14	120	0.36	1.06	59	Straw	0.1	0.0	0.0
SU3	0.13	117	0.23	0.96	0		7.5	3.2	0.1
SU4	0.37	168	0.39	2.20	0		6.1	0.5	0.0
SU5	1.58	261	0.10	9.37	0		1.9	0.4	0.0
SU6	1.23	173	0.11	8.51	0		2.3	0.5	0.0

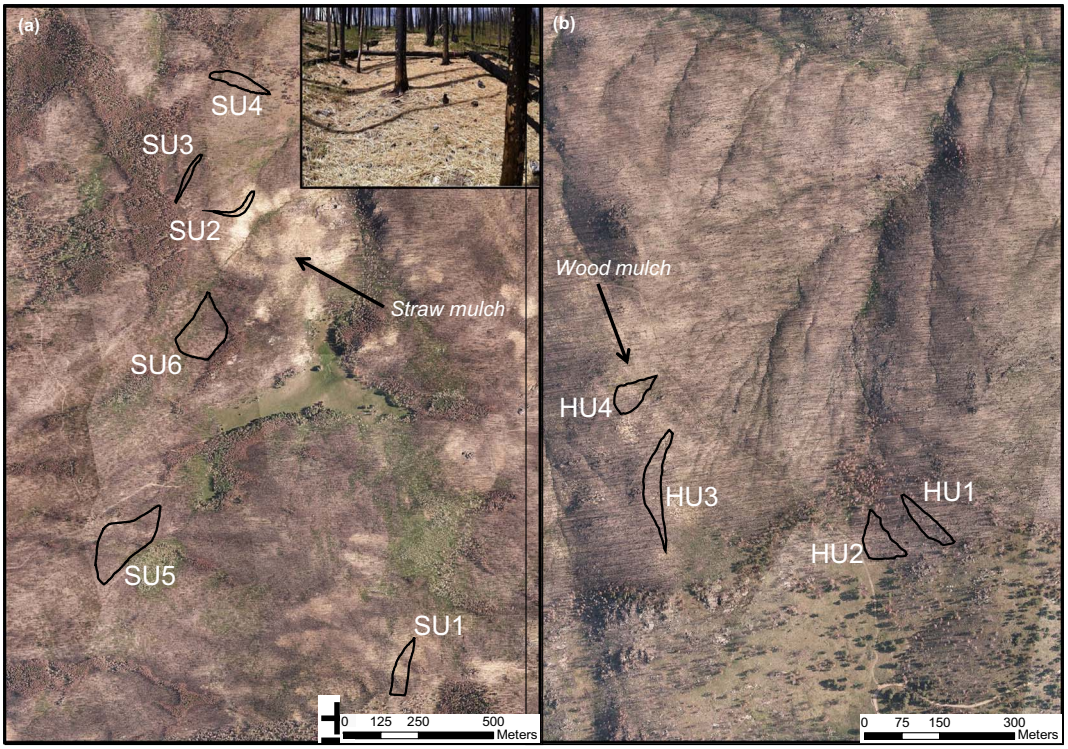

Fig. 2. Contributing areas to sediment fences in mulched clusters in upper Skin Gulch (SU, a) and upper Hill Gulch (HU, b) over 2013 aerial photography from the National Ecological Observatory Network Airborne Observation Platform. Inset photo in (a) shows straw mulch at SU2 shortly after application in 2013.

between the unmulched and mulched subsets. We considered only annual total *SY* for this analysis; event-scale *SY*s are presented in Schmeer (2014) and Kampf et al. (2016).

To examine the variables affecting hillslope erosion, we identified a series of time-varying (ground cover, rainfall) and static (topographic) variables describing each hillslope (Table 2). For ground cover, we used the values of percent bare soil, percent live vegetation, percent litter, and percent mulch at the beginning of the growing season. Ground cover changed during each growing season, but we only used the value at the beginning of the growing season because this was most consistent with our goal of developing erosion prediction models. For rainfall, we summarized growing season (June–October) total precipitation (*P*) and total 30-minute rainfall erosivity (EI_{30}) for each rain gauge. EI_{30} was calculated using the Rainfall Intensity Summarization Tool (RIST) program from the Agricultural Research Service (ARS, 2013), which applies the Brown and Foster (1987) equation for kinetic energy and multiplies this by maximum 30-minute storm intensity to obtain the EI_{30}. We selected these rainfall variables because they integrate over time, in contrast to event-specific variables such as maximum rainfall intensities.

Table 2
Abbreviations and descriptions of the independent variables evaluated for their relationship with sediment yields (*SY*) from the High Park Fire.

Variable	Description	Type
%*B*	% of hillslope area with bare soil (unitless)	Cover
%*V*	% of hillslope area with vegetation ground cover (unitless)	Cover
%*L*	% of hillslope area with litter ground cover (unitless)	Cover
%*M*	% of hillslope area with mulch cover (unitless)	Cover
P	Jun–Oct precipitation depth (mm)	Rainfall
EI_{30}	Jun–Oct 30-minute rainfall erosivity (MJ mm ha^{-1} h^{-1})	Rainfall
S	Average of all pixel slopes in hillslope area (m/m)	Topographic
L	Length of longest flow path in hillslope area (m)	Topographic
W	Contributing area divided by *L* (m)	Topographic
W/L	Width to length ratio (unitless)	Topographic
TI	Maximum value of the topographic index in hillslope area (unitless)	Topographic

We derived static topographic variables from a 0.75 m resolution digital terrain model developed using LiDAR data collected by the Federal Emergency Management Agency (FEMA) in fall 2013. For each hillslope area we computed five topographic metrics: slope (*S*), longest flow path length (*L*), average width (*W*), width to length ratio (*W/L*), and maximum topographic index (*TI*). For *S* we used the average slope for all cells within the hillslope contributing area, and for *L* we used the longest length of a flow path within the hillslope as computed with a D8 flow direction algorithm, which routes flow from each cell in one of eight directions based on steepest descent. We computed *W* as drainage area (*A*) divided by *L* and *TI* as ln(*A/S*) (Beven and Kirkby, 1979). For each hillslope we identified the maximum *TI* value. All topographic variables were derived using RiverTools (Rivix LLC, 2004).

To evaluate controls on *SY*, we first conducted pairwise correlation analysis between each independent variable and log(*SY*). *SY* was log transformed for this analysis because the values were not normally distributed. Next, we developed a simple empirical model structure and used statistical techniques to study and characterize its performance. The empirical model describes *SY* as being proportional to the product of one cover, one rainfall, and one topographic variable in the form:

$$SY = K * Cover * Rainfall * Topographic \quad (1)$$

where *SY* is the annual sediment yield; the cover, rainfall, and topography variables can be any of the variables listed in Table 2, and *K* is an empirical coefficient. We statistically analyzed this model structure to determine the best choice of variables, and we compared the simple empirical model to a more complicated, general power law relationship that has the form:

$$SY = K_1 + K_2 \times (Rainfall^{\alpha} \times Cover^{\beta} \times Topographic^{\gamma}) + \varepsilon \quad (2)$$

where K_1 is an additive shift that adjusts for overall bias in the

Table 3
Summary of the measured hillslopes from the fires used to test the erosion prediction models developed for the High Park Fire.

Fire	Month and year of burn	Number of hillslopes	Years of data	Area range (ha)	Length range (m)
Big Elk	August 2002	3	4	0.08–0.4	140–240
Bobcat	June 2000	48	5	0.01–5	30–500
Crosier	September 1998	5	4	0.04–1	70–400
Dadd Bennett	January 2000	5	3	0.02–5	30–500
Hewlett	April 2002	3	3	0.08–0.2	110–130
High Park	June 2012	29	3	0.08–1.6	50–270

empirical model (Eq. (1)). Statistical analysis determines the powers (α, β, and γ) and empirical coefficient (K_2) values that minimize the average prediction error (ε) for each combination of variables. We evaluated a power law model instead of a multiple regression model because the power law directly models *SY* and does not, like multiple regression models, rely on transformations of data to make predictions and quantify uncertainties. Since Eq. (2) is not a standard linear model, we used Bayesian methods to estimate model parameters (Gelman et al., 2004). We used the Bayesian version of confidence intervals, the credible interval, to report the uncertainty in our power and coefficient estimates and report the R^2 and the deviance information criteria (DIC). The DIC is a relative, unitless measurement of predictive power that is sensitive to model complexity (Gelman et al., 2004). An R code for this analysis is included in the supplementary materials.

Based on our initial analysis of the models in Eqs. (1) and (2) and on the types of data likely to be most readily available after fires (daily precipitation rather than shorter time intervals), we selected the empirical models that would be most appropriate for future applications. For these models we also computed the Nash Sutcliffe Coefficient of Efficiency (NSCE) and the relative root mean squared error (rRMSE).

3.3. Model testing

We tested the selected empirical models using erosion data from other fires in the region to evaluate model performance on fires not used in model development (Table 3); additional descriptions of these fires are available in Benavides-Solorio and MacDonald (2005), Pietraszek (2006), and Larsen and MacDonald (2007). These sites were selected because they are all within the footprint of the FEMA LiDAR topographic data used for High Park Fire analysis. For each fire, we had GPS coordinates available for sediment fence locations, and using these locations we delineated the hillslope contributing area using the 0.75 m DEM and the D8 algorithm. GPS locations were not always very precise, so some subjective judgement was needed to identify outlet pixels for delineating contributing areas. This was most difficult for planar hillslopes or convergent hillslopes that intercepted multiple flow pathways. For one site at Bobcat and three sites at Big Elk Fire, the GPS locations had no clear relationship to the flow pathways derived from the DEM, so we excluded those hillslopes from the analysis. The derived contributing areas were used to determine values of *L*, *W*, and *TI* for each hillslope.

Data summaries for the test fires report percent ground cover; to link these values with our model structure, we estimated percent bare soil (%*B*) as 100 - percent cover. We computed June–October total precipitation (*P*) using values from the nearest rain gauge in the fire monitoring area. Because these were research sites, rain gauges were usually located close to the erosion monitoring locations, but there were some data gaps, particularly in early June and October. We filled gaps using other rain gauges in the same fire area when possible. If no rain gauge data were available within the fire area, we used daily precipitation values from PRISM (http://prism.oregonstate.edu) to fill in the missing values. The amount of infilling required varied by fire: 0% of days at High Park Fire, 14% at Crosier, 19% at Dadd Bennett, 21% at Bobcat, 34% at Big Elk, and 43% at Hewlett. Through ongoing research in this region, we have found that PRISM precipitation values are usually consistent with rain gauge values. We compiled annual *SY* data from all sites starting the year after the fire (year 1), again excluding all *SY* data for year 0 because most of the data sets for the year of the fire were incomplete. Using the values of *L*, %*B*, and *P*, we applied both Eq. (1) and Eq. (2) models to predict *SY* and evaluated the predictions using NSCE and rRMSE.

4. Results

4.1. High Park Fire ground cover, rainfall, and sediment yield

The hillslopes in the High Park Fire averaged 57% bare soil in the first few months after the fire, with < 3% live vegetation. Average percent bare soil only declined to 54% by the beginning of the 2013 growing season, as most of the increase in live vegetation was counteracted by a decrease in the underlying litter (Fig. 3). Mulch applications in 2012 and early 2013 added 20–66% mulch cover to eight

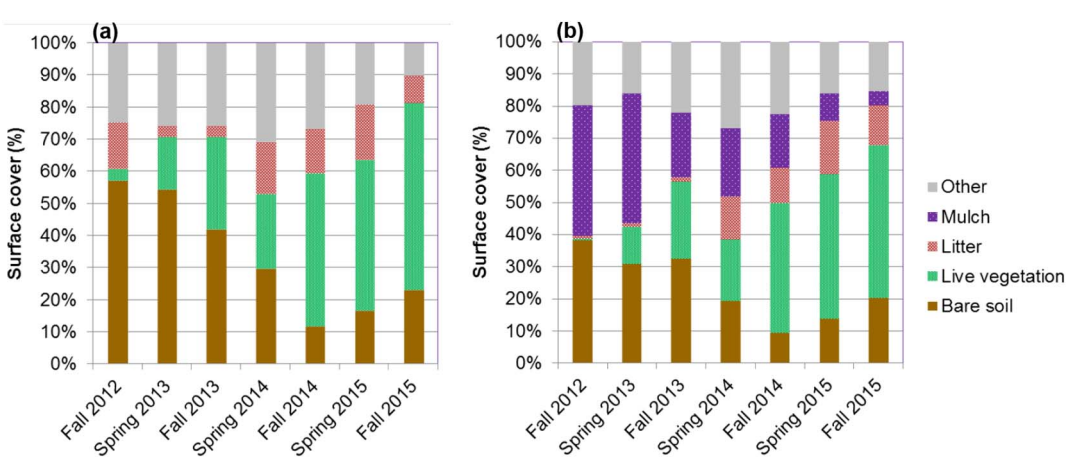

Fig. 3. Average percent surface cover over time for (a) unmulched hillslopes and (b) mulched hillslopes in the High Park Fire. The "other" category includes tree, wood, and rock.

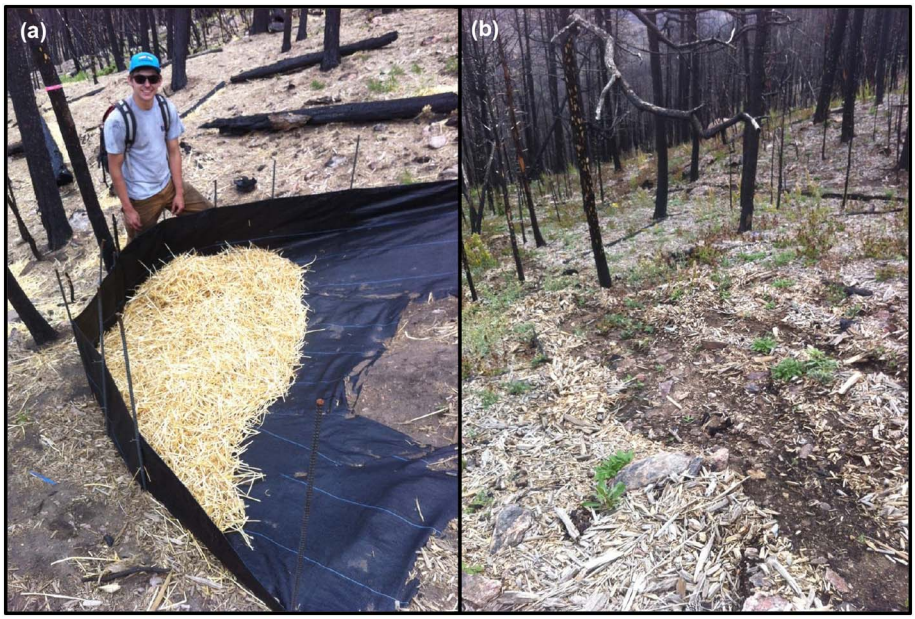

Fig. 4. Mechanisms of mulch loss from hillslopes in the High Park Fire: (a) wind-blown straw mulch trapped in a sediment fence, and (b) rills formed through wood shred mulch in HU after a large storm in September 2013.

hillslopes (Table 1). For those eight hillslopes, mean mulch cover at the beginning of the 2013 growing season was 40%, and mean bare soil was 31%.

During the 2013 growing season, bare soil declined to 42% on average at unmulched hillslopes mostly due to an increase in vegetation cover from 16% at the beginning of the season to 29% on average at the end of the growing season (Fig. 3). On mulched hillslopes, mulch cover declined to an average of 20% cover by the end of the 2013 growing season. This was due to a combination of wind and overland flow (Fig. 4) and potentially some under-counting where vegetation had grown over the mulch. We found no apparent difference in the rates of mulch decline for hillslopes with different types of mulch. In 2013 average vegetation cover on mulched hillslopes also increased from 12% at the beginning of the growing season to 24% at the end of the growing season.

During 2014 and 2015, live vegetation gradually increased on unmulched hillslopes to an average of 59% at the end of the 2015 growing season (Fig. 3). Mean percent bare soil declined in 2014 to 12% and then increased to 16% in 2015. Observers conducting ground cover counts varied between years, and we do not know whether the reported increase in bare soil in 2015 is real or a result of observer bias. However, other studies in the fire also documented an increase in bare soil from 2014 to 2015 (J. Giordanengo, AloTerra, unpublished data), possibly because of the drier conditions in 2015. The amount of mulch continued to decline in 2014 and 2015, and by the end of the 2015 growing season mean mulch cover was only 5%. The mulched hillslopes started the 2014 season with lower bare soil (19%) than unmulched hillslopes (30%), but by fall 2014 both unmulched and mulched hillslopes had similar amounts of bare soil.

The year after the fire, 2013, was a relatively wet year, with 462 mm of rainfall on average from Jun to Oct (Table 4). Much of this rain fell during an unusually large rain storm in September 2013 that contributed 250–280 mm of rain to the hillslopes. Subsequent years after the fire, 2014 and 2015, were drier, with 266 mm and 194 mm average growing season precipitation, respectively. Erosivity was also highest in 2013 and lower in 2014 and 2015. On average, June–October 2013 contributed 50% of the P and 59% of the EI_{30} accumulated over all three summers combined.

Sediment yield was highest in 2013, with an average of 12.1 Mg ha^{-1} on unmulched hillslopes and 3.1 Mg ha^{-1} on mulched hillslopes (Table 4), a factor of four differences. In 2014 and 2015 SY declined substantially. Average SY in 2014 was 1.1 Mg ha^{-1} on unmulched hillslopes compared to 0.3 Mg ha^{-1} on mulched hillslopes, a difference of about a factor of three. By 2015, only trace amounts of sediment were collected at the studied hillslopes except during one large rain storm on August 16. This rain storm primarily affected Hill Gulch and produced small debris flows at HL5, HL 6 and HU3. These three hillslopes were all mulched hillslopes, so the mean SY's from the mulched hillslopes in 2015 (0.4 Mg ha^{-1}) were higher than the unmulched hillslopes (0.0 Mg ha^{-1}).

Overall, 2013 accounted for 93% of the total SY on unmulched hillslopes and 87% of the total on mulched hillslopes. The 'SYs in 2013 were significantly different from those in 2014 and 2015 ($p < 0.0001$, t-test), but the 'SYs in 2014 were not significantly different from those in 2015. 'SYs in mulched hillslopes were significantly different from unmulched hillslopes in 2013 ($p = 0.02$) and 2015 ($p = 0.01$), but not in 2014.

4.2. Independent variable correlations with log(SY)

The time-varying variables, cover and rainfall, had the highest correlations with log(SY) (Table 5). Cover variables were all significantly correlated with one another ($r = -0.64$ to 0.40), and all except mulch (%M) were significantly correlated with log(SY). Percent bare soil (%B) had the strongest correlation with log(SY) ($r = 0.76$), likely because this variable integrates the effects of the other three cover variables. With one exception, hillslopes did not produce much sediment unless they had at least 25% bare soil (Fig. 5a).

The rainfall variables, P and EI_{30}, were significantly correlated with one another ($r = 0.87$) and with log(SY) ($r = 0.73$ and 0.68, respectively; Table 5), with the highest correlation for total precipitation (P).

Table 4
Mean growing season (Jun-Oct) precipitation variables from 2013 to 2015 and mean total sediment yield (SY) for unmulched and mulched hillslopes in the High Park Fire. The values in parentheses are standard deviations.

Year	P (mm)	EI_{30} (MJ mm ha^{-1} h^{-1})	SY unmulched (Mg ha^{-1})	SY mulched (Mg ha^{-1})
2013	462 (34)	1415 (287)	12.1 (8.7)	3.1 (3.1)
2014	266 (41)	663 (312)	1.1 (1.9)	0.3 (0.4)
2015	194 (30)	353 (279)	0.0 (0.0)	0.4 (0.6)
Total	921 (55)	2431 (802)	13.2 (10.2)	3.8 (3.8)
% from 2013	50 (1)	59 (7)	93 (9)	87 (13)

Table 5
Pairwise correlations between independent variables and log-transformed sediment yield, log(*SY*). Values in bold are significant ($p < 0.05$). See Table 2 for full variable names.

	Bare %*B*	Live veg %*V*	Litter %*L*	Mulch %*M*	Precip *P*	Erosivity EI_{30}	Slope *S*	Length *L*	Width *W*	*W/L*	Index *TI*
%*V*	**−0.64**										
%*L*	**−0.56**	**0.40**									
%*M*	**−0.22**	**−0.35**	**−0.23**								
P	**0.71**	**−0.69**	**−0.69**	0.20							
EI_{30}	**0.64**	**−0.71**	**−0.67**	**0.37**	**0.87**						
S	**−0.21**	0.10	0.04	−0.17	0.02	−0.04					
L	0.06	−0.03	0.16	−0.18	0.07	−0.17	0.15				
W	0.09	−0.02	0.11	−0.09	0.02	−0.08	**−0.34**	**0.62**			
W/L	−0.01	0.04	−0.02	0.09	−0.06	0.09	**−0.45**	**−0.31**	**0.49**		
TI	0.20	−0.01	0.06	−0.17	0.03	−0.11	**−0.38**	**0.71**	**0.92**	**0.28**	
logSY	**0.76**	**−0.52**	**−0.58**	−0.18	**0.73**	**0.68**	0.04	−0.11	−0.08	0.06	−0.08

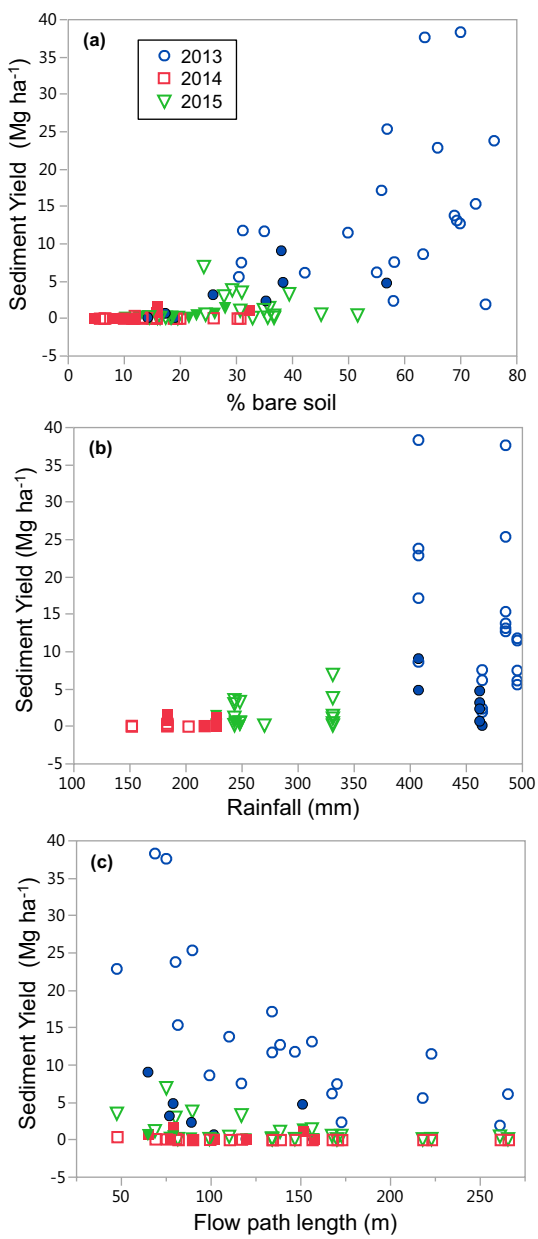

Fig. 5. Relationships between annual sediment yields (*SY*) for each hillslope and a) percent bare soil in spring (%*B*), b) June–October rainfall (*P*), and c) longest flow path length (*L*). Open symbols are unmulched or sparsely mulched (< 5% mulch cover) hillslopes, and filled symbols are mulched hillslopes (> 20% mulch cover).

Precipitation variables were also significantly correlated with cover variables (r = −0.71 to 0.71), largely because the year with highest precipitation (2013) was the year with the lowest ground cover. The differing amounts of precipitation for each year are clearly evident in a scatter plot (Fig. 5b). Most of the topographic variables were significantly correlated with one another, but none of them were significantly correlated with log(*SY*) (Table 5). The highest correlation coefficients between topographic variables and log(*SY*) were for *L* (r = −0.11; Fig. 5c), *W* (r = −0.08), and *TI* (r = −0.08).

4.3. Models of annual SY

All combinations of the cover, rainfall, and topographic variables listed in Table 2 were tested using the power law equation (Eq. (2)) and the High Park Fire *SY* values. The coefficients, confidence intervals, and performance statistics for the best models are presented in Table 6. Percent bare soil is consistently the best cover variable to use. The DIC and R^2 model comparison statistics show no strong preference for using one precipitation variable instead of the other. For topographic variables, despite *L* being marginally more correlated with log(*SY*) than *TI* (Table 5), the predictions using *TI* in the empirical model tended to be better. The top two models use the same cover (%*B*) and topographic variable (*TI*) and have nearly identical predictive performance despite using different precipitation variables. Models 3 and 4 in Table 6 also support this conclusion since these two models have effectively identical performance using different precipitation variables.

Some of the credible intervals for the exponents α or β in models 2, 3, 6, and 7 do not include 1 or −1, which suggests power law relationships are needed for predicting *SY* with these variables. The exponent credible intervals for models 1, 4, and 5 do include 1 or −1, so these models should make predictions that are largely consistent with Eq. (1). Fig. 6 presents examples of the predicted ranges of *SY* values for models 1 and 4. Many of the prediction ranges intersect the 1:1 line, indicating the model can reasonably predict *SY*s less than around 17 Mg ha^{-1}, but the prediction ranges tend to fall below the 1:1 line when *SY* is > 17 Mg ha^{-1}.

Since model performance is not greatly affected by the choice of precipitation or topographic variables, we recommend using the model from Table 6 that has *P* and *L* as input variables (model 4). We recommend *P* because this value is most easily obtained for other study areas, whereas EI_{30} requires precipitation data with at least 30-minute resolution. For the topographic variable, we recommend *L* because *TI* values are more sensitive to the spatial resolution of topographic data (Hastings and Kampf, 2014). Furthermore, based on the credible intervals of exponents, model 4 should make predictions that are largely consistent with the simpler empirical model (Eq. (1)). This leads to the following empirical model:

$$SY = K\,(P{*}\%B{*}L^{-1}) \tag{3}$$

The value of the empirical coefficient, *K*, can be derived as the slope

Table 6
Estimated coefficients, 95% credible intervals, and model fit statistics for highest ranking combinations of rainfall, cover, and topographic variables (Table 2) for predicting *SY* at the High Park Fire using the Eq. (2) power law relationship. Models are listed in order of increasing deviance information criteria (DIC). An estimate of the standard deviation *SD* of the model error term ε in Eq. (2) is also included.

Model	K_1	$K_2 \times 1000$	α		β		γ		Error	Fit	
	Est. (95% CI)	Est. (95% CI)	Var.	Est. (95% CI)	Var.	Est. (95% CI)	Var.	Est. (95% CI)	$SD(\varepsilon)$	R^2	*DIC*
1	− 0.07 (− 1.7, 1.5)	0.23 (0.0, 1.7)	EI_{30}	0.81 (0.44, 1.3)	%*B*	1.3 (1.0, 1.7)	*TI*	− 0.83 (− 1.0, − 0.65)	3.1	0.84	468
2	− 0.08 (− 1.8, 1.6)	0.08 (0.0, 1.6)	*P*	0.99 (0.31, 1.6)	%*B*	1.5 (1.1, 1.9)	*TI*	− 0.83 (− 1.0, − 0.66)	3.2	0.84	477
3	− 0.05 (− 2.0, 1.8)	33 (0.01, 360)	EI_{30}	0.62 (0.15, 1.1)	%*B*	1.5 (1.1, 2.0)	*L*	− 1.0 (− 1.3, − 0.75)	3.8	0.77	504
4	− 0.05 (− 2.0, 1.9)	5.6 (0.0, 220)	*P*	1.1 (0.16, 1.9)	%*B*	1.5 (1.0, 2.0)	*L*	− 1.1 (− 1.4, − 0.83)	3.7	0.78	504
5	0.0 (− 2.1, 2.0)	9.8 (0.02, 120)	EI_{30}	0.73 (0.20, 1.3)	%*B*	1.2 (0.77, 1.8)	*W*	− 1.1 (− 1.5, − 0.65)	4.1	0.73	521
6	− 0.06 (− 1.8, 1.8)	0.03 (0.0, 0.33)	EI_{30}	1.9 (1.4, 2.3)	%*L*	0.02 (0.0, 0.05)	*TI*	− 1.1 (− 1.3, − 0.79)	4.3	0.70	522
7	− 0.07 (− 2.2, 2.0)	0.81 (0.0, 9.0)	EI_{30}	0.34 (− 0.24, 0.93)	%*B*	2.1 (1.4, 2.7)	*S*	1.0 (0.62, 1.5)	4.1	0.74	523

of the best fit line between *SY* (y axis) and $(P * \%B * L^{-1})$ (x axis). Values of *K* are unit-dependent; in our application Jun–Oct precipitation (*P*) is in mm, and *L* is in m. The model for the High Park Fire in Eq. (3) has a *K* value of 0.06, NSCE of 0.70, and rRMSE of 1.1 Mg ha^{-1}. It over-predicts the low '*SY*s and tends to under-predict the highest *SY*s but generally provides a reasonable fit to the observed values (Fig. 7b,d).

We tested the empirical model (Eq. (3)) and its power law counterpart (model 4, Table 6) for predicting annual *SY* at the other test fires. At all fires, the models tend to over-predict low '*SY*s (Fig. 7), and this is particularly evident when the data are plotted on a log scale (Fig. 7c,d). While the models performed reasonably well for *SY* predictions at High Park Fire (NSCE 0.70–0.72; rRMSE 1.0–1.1; R^2 0.75–0.76), the location for which they were developed, their performance declined when evaluating the test fires (NSCE 0.26–0.32; rRMSE 1.9–2.0; R^2 = 0.29–0.33) (Table 7). This performance was mostly due to the large number of observations at the Bobcat Fire (n = 158), and model performance for the Bobcat fire alone was similar to performance for all test fires combined. For the Big Elk Fire, the model '*SY*s were highly correlated with observations (R^2 = 0.51–0.68), but they were lower than the observed values in most cases. For the other three fires, model performance was poor (NSCE < 0; rRMSE ≥ 15; $R^2 \leq 0.02$). These fires all had low sample sizes, and '*SY*s did not correlate with all of the variables in the model. At Crosier (n = 19) *SY* was only significantly correlated with *P* (R^2 = 0.22). At Hewlett Gulch (n = 9) *SY* was significantly correlated with percent bare soil (R^2 = 0.73) and *P* (R^2 = 0.23), but the correlation with *P* was negative rather than positive. At Dadd Bennett (n = 15) *SY* was only significantly correlated with percent bare soil (R^2 = 0.31).

5. Discussion

5.1. Ground cover and effects of mulch

Our findings here confirm those reported in previous studies, indicating that the bare soil or its inverse (ground cover) is a strong control on rates of annual post-fire erosion (Benavides-Solorio and MacDonald, 2001, 2005; Wagenbrenner et al., 2006; Larsen et al., 2009; Robichaud et al., 2013a). We did not consider burn severity explicitly as a control on *SY* because soil burn severity is directly related to percent bare soil (Benavides-Solorio and MacDonald, 2005). On the High Park Fire, bare soil declined to around 20% or less by the end of the 2014 growing season, and this is likely a key reason why erosion rates were generally < 1 Mg ha^{-1} during 2014 and 2015, the second and third years after the 2012 fire. Increase in live vegetation cover caused most of the decline in bare soil, and rates of vegetation recovery were similar to other fires in the region except those on the coarse-textured soils derived from Pikes Peak granite (Benavides-Solorio and MacDonald, 2005; Wagenbrenner et al., 2006; Wagenbrenner et al., 2015).

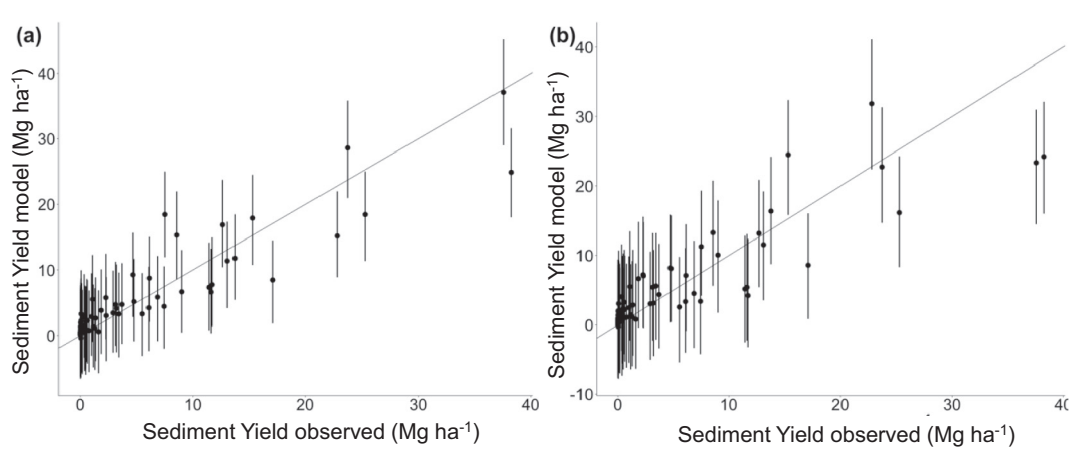

Fig. 6. Predicted vs. observed annual *SY* for statistical models 1 (a) and 4 (b) from Table 6. Points are predictions using median values of the model coefficients, and bars show the credible intervals. 1:1 line shown for reference.

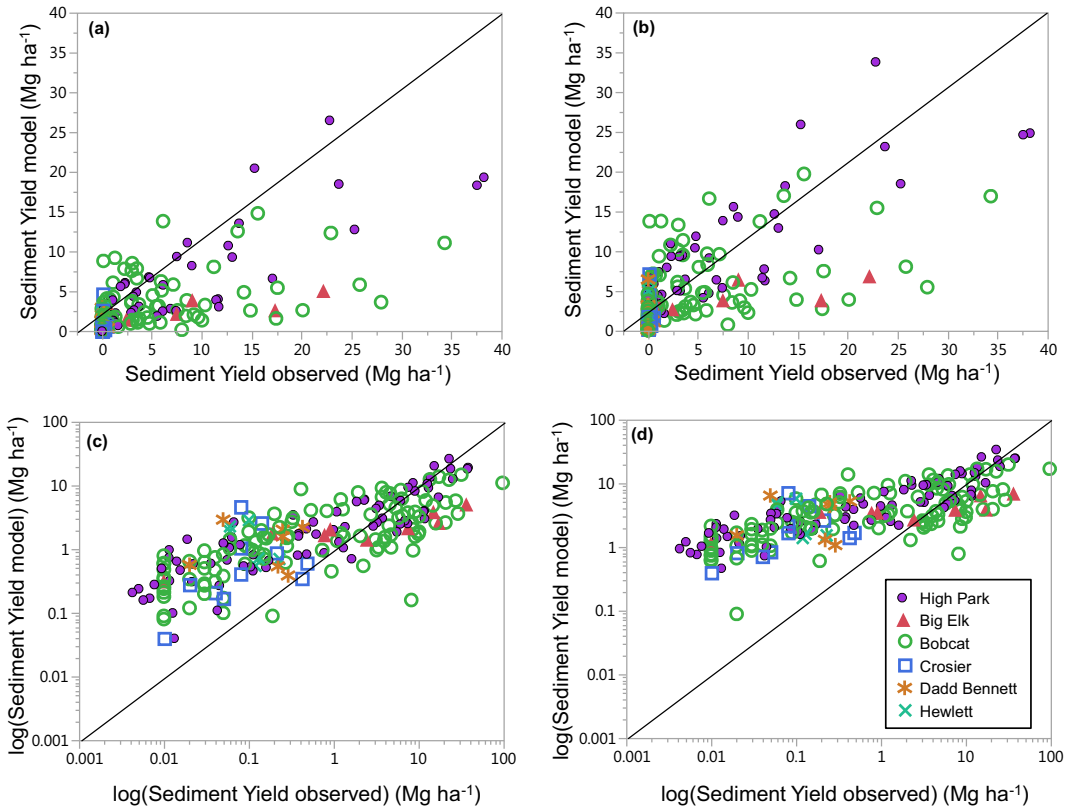

Fig. 7. Predicted vs. observed annual *SY* and log(*SY*) for High Park Fire and test fires using the power law model 4 (Table 6) (a, c) and the empirical model (Eq. (3)) (b, d) plotted on both arithmetic (a, b) and log scales (c, d). 1:1 line shown for reference.

Table 7
Performance statistics for a power law model and an empirical model that use %*B*, *P*, and *L* to predict *SY* at test fires. Performance of the models at High Park Fire, the fire for which they were developed, is included for reference.

Group	Power law model (Table 6, model 4)			Empirical model (Eq. (3))		
	NSCE	rRMSE	R^2	NSCE	rRMSE	R^2
High Park Fire	0.72	1.0	0.76	0.70	1.1	0.75
All Test Fires	0.32	1.9	0.33	0.26	2.0	0.29
Bobcat	0.32	1.7	0.33	0.27	1.8	0.30
Big Elk	− 0.08	1.2	0.68	0.13	1.1	0.51
Crosier	− 101	15	0.02	− 321	26	0.01
Dadd Bennett	− 677	26	0.00	− 4033	64	0.00
Hewlett Gulch	− 309	16	0.02	− 1550	36	0.01

Mulching reduced the bare soil cover by an average of 44% during 2013, the first year after the fire, and this corresponded with a factor of four lower *SY* than in the unmulched hillslopes. The mulch cover declined by > 50% in 2013, but *SY* on mulched hillslopes was still a factor of three lower than the unmulched hillslopes in the following year (2014). By 2015, mulched and unmulched sites had similar amounts of bare soil, and the effects of mulch on *SY* were no longer evident.

The large storm in September 2013 might have caused more loss of mulch than would have occurred in drier conditions, as indicated by rilling in the wood mulch (Fig. 4b) and the large quantities of wood mulch in the sediment fences after this storm. Field observations suggest that the wood mulch was much more persistent outside of the primary rills. Surprisingly, hillslopes with dense straw mulch did not exhibit similar rilling. However, our sample size was small, and the effectiveness of different mulch types varies by location and timing of mulch application relative to large storms (Wagenbrenner et al., 2006). Some studies have reported that wind is more likely to displace straw mulch, causing it to decline faster that wood mulch (Robichaud et al., 2013b), whereas at other study sites straw persisted more than wood because it adhered to the soil (Fernandez et al., 2011).

5.2. Rainfall

An important finding from our model development and testing is that at the annual time scale, empirical models could predict *SY* using either total precipitation (*P*) or erosivity (EI_{30}). The ability to predict *SY* using *P* alone is convenient because of greater availability of daily precipitation data from weather stations and spatial products such as PRISM (http://prism.oregonstate.edu).

Distinguishing the effects of rainfall on *SY* from those of other controlling variables is somewhat impaired in this study by the large differences in rainfall between years and the high correlation between rainfall and bare soil. For the High Park Fire, 2013 had by far the highest rainfall as well as lowest ground cover (highest bare soil). To separate out the effects of rainfall and bare soil, we computed the *SY* per mm of rainfall in each year. On average, this value was highest in 2013 (0.03 Mg ha^{-1} mm^{-1}) and declined by an order of magnitude to 0.003 Mg ha^{-1} mm^{-1} in 2014 and to 0.001 Mg ha^{-1} mm^{-1} in 2015. This decline indicates that bare soil alone has a strong and temporally consistent influence on *SY*. The combination of high rainfall and high bare soil in 2013 meant *SY*s in 2013 dominated the total measured post-fire hillslope erosion.

5.3. Topography

Although percent bare soil and rainfall were the two dominant controls on *SY*, topography also affected erosion rates. Surprisingly slope had the weakest correlation to *SY*, which may be because the studied hillslopes are all relatively steep (mean 38%, standard deviation

13%). *L*, *W*, *W/L*, and *TI* also had weak, non-significant univariate correlations with *SY*, but at least one of these topographic variables was needed to maximize empirical model performance (Eqs. (1)–(3)). The topographic variables were poorly correlated with the cover and precipitation variables ($R^2 < 0.04$) except for the relationship between bare soil and slope (Table 5), so the addition of a topographic variable added unique value to the multivariate modeling.

The absolute decline in *SY* with increasing slope length is opposite to the relationship assumed in the Revised Universal Soil Loss Equation (RUSLE), in which *SY* increases with slope length. The difference in the direction of the relationship may be because many of the studied hillslopes are outside the range of lengths recommended for applications of USLE (< 120 m; Wischmeier and Smith, 1978; Renard et al., 1997), and generally the studied slopes are long enough that concentrated channelized flow may dominate over rainsplash, sheetwash, and shallow rilling. Prior simulations with a more physically-based model, Disturbed WEPP, indicated that erosion increases with slope length in a wet climate, whereas in a drier climate like our study area, erosion rates increase with slope length up to about 200 m then decline as hillslope lengths exceed 250 m (Miller et al., 2011). Some of our studied hillslopes were longer than 200 m (Table 1), but the steepest decline in *SY* with slope length was for shorter hillslopes (< 130 m; Fig. 5c). This decline with length may be due to the nature of the overland flow hydrographs, which had rapid recession limbs that may have caused mobilized sediment to be deposited before reaching hillslope outlets.

The general trend of declining '*SY*s with greater flow path length is consistent with declining unit area *SY* with greater contributing areas found in multiple studies (Mayor et al., 2011; Wagenbrenner and Robichaud, 2014; Prats et al., 2016). However, other studies have documented increasing sediment yields from hillslopes to larger watershed scales (Moody and Martin, 2009). These differences in findings about how *SY* changes with spatial scale highlight the complexity of erosion and deposition processes along flow paths. Models such as RUSLE that were developed with data from a limited range of spatial scales may not be appropriate for erosion prediction at coarser spatial scales. Similarly, the hillslope-scale empirical models developed here for predicting sediment yields may not be transferable to either finer or coarser spatial scales.

5.4. Annual SY models

The empirical *SY* models developed for the High Park Fire using percent bare soil plus a precipitation and a topographic variable had relatively strong performance (R^2 0.70–0.84). These values are in the range of other site-specific multiple linear regression models of post-fire *SY* (R^2 = 0.58–0.83, Benavides-Solorio and MacDonald, 2005; Pietraszek, 2006). Notably, all of our empirical models use just percent bare soil (%*B*) as the cover variable. This single variable correlates with live vegetation, litter, mulch, rock or any other cover. Consequently predictive *SY* models generally should not need to include other cover variables, burn severity, or time since burning. Using percent bare soil also allows both mulched and unmulched hillslopes to be represented in a single erosion model. While the models we developed are empirical, conceptually the combination of rainfall and bare soil represents both the amount of infiltration excess overland flow and the susceptibility of a given soil to erosion caused by varying levels of surface disturbance.

Empirical model performance declined substantially when applied to the test fires, which is not surprising because they were fit directly to the High Park Fire data. However, without any model calibration these models did have positive NSCE values (0.26–0.32) for all fires grouped together and represent an improvement over hillslope-scale predictions for the same fires using the more detailed RUSLE (NSCE = 0.06) and Disturbed WEPP (NSCE = 0.19) models (Larsen and MacDonald, 2007). The empirical models do have the problem of under-predicting small soil losses that has been documented elsewhere (Nearing, 1998), but this problem is improved somewhat when using the power law forms of the models (Eq. (2)). Nearing (1998) demonstrated that model biases can be caused by natural variability not represented in a deterministic model, and he suggested that perfect model performance should not be expected from a deterministic erosion model. Further problems with the empirical models are uncovered when examined for individual fires. The models performed poorly at some fires (Big Elk, Crosier, Dadd Bennett, Hewlett), which may mean these models are not transferable to all fires in the region. However, the fires with poor model performance also had ≤ 5 monitored hillslopes; with a sample size this small, the dominant trends relating ground cover, precipitation, and topography to sediment yield can be masked by the high variability in individual hillslope characteristics and *SY*s. All of the fires tested have *SY*s within the range of values predicted for High Park and Bobcat fires, where sample sizes were much higher and the models performed better (Fig. 7).

The final recommended model we developed (Eq. (3)) has a structure that is analogous to RUSLE (Renard et al., 1997) in that it multiplies the key controlling variables. The major difference with RUSLE is that our model uses only three directly measurable input variables (%*B*, *P*, *L*) rather than the empirical transformations of rainfall, cover, and topographic variables required to apply RUSLE. No empirical model is needed to derive values for *K*, the model coefficient in Eq. (3). However, at this stage we have no basis for determining the value of *K* a priori, and because the model is empirical it may only be applicable to conditions similar to those of the High Park Fire.

5.5. Uncertainties

Each of the variables we measured at the High Park Fire has some uncertainty. Ground cover was measured by point transects, which can be affected by transect placement and observer bias. Rainfall data are affected by catch efficiency and spatial variability of rainfall not captured by the gauge network, particularly for the summer convective storms that cause most of the post-fire erosion in the study area. Gap filling of precipitation values also introduced additional uncertainty at the test fires. Values of topographic variables are sensitive to the accuracy of determining sediment fence locations, and there were usually discrepancies between visual field delineations of hillslope boundaries and those computed with digital elevation data. Uncertainties in drainage area also affect accuracy of sediment yields. At test fires, coordinates for sediment fence locations were less precise than those for High Park Fire, and this may have contributed to greater uncertainties in both *SY* and values of *L*. Finally, the sediment fence data themselves probably underrepresent *SY*, both because the fences occasionally overtopped with sediment and also because the fences do not capture all suspended sediment.

The empirical model development and application excluded sediment yield data from the year of the fire, so we do not know whether the models will accurately predict erosion in year 0. Data gaps in year 0 are a problem for most post-fire model evaluations because it is difficult to get monitoring equipment in place soon enough after the fire to capture all erosion in year 0. We also did not consider other potential controlling variables such as soil texture, soil structure and depth, bedrock outcrops, soil water repellency, canopy cover, and soil moisture (Neary et al., 1999; Huffman et al., 2001; Shakesby and Doerr, 2006). Accurate soil characteristics are particularly difficult to determine because soil survey data are coarser resolution than individual hillslopes and based on limited field samples. Field samples of soil texture at High Park Fire sites showed little relationship to *SY* (Schmeer, 2014), and may not have been representative of the entire hillslope area. Near-surface soil texture can also be time-varying because as fine particles are eroded from the surface, eroded areas may become armored (Morris and Moses, 1987; Schaffrath, 2009). Other soil properties, such as soil moisture and soil water repellency, will vary over time, indicating that multiple measurements of soil properties over

time and space are needed to represent post-fire soil conditions accurately.

6. Summary and conclusions

Annual hillslope erosion after the 2012 High Park Fire was over 12 Mg ha^{-1} on average during the first full summer after the fire (2013), when both rainfall and bare soil were highest. Sediment yields declined to ≤ 1 Mg ha^{-1} during the second and third years post-fire. Percent bare soil was the strongest control on annual sediment yield. Mulch decreased the amount of bare soil, and mulched hillslopes had a four-fold reduction in sediment yield in the first year after the fire, with no apparent difference in mulch effectiveness between straw and wood chips. The effectiveness of mulch in reducing erosion declined over time, and by the third year after the fire, mulched and unmulched hillslopes had similar erosion rates. Total rainfall and rainfall erosivity were both highly correlated with annual *SY*, whereas topographic variables were only weakly correlated to *SY*.

We found that empirical models can predict annual hillslope-scale *SY* at the High Park Fire using only percent bare soil combined with one precipitation variable (*P* or EI_{30}) and one topographic variable (*L* or *TI*) (R^2 = 0.70–0.84). Model performance was not strongly affected by the choice of precipitation or topographic variable, so we recommend using models that predict *SY* as a function of percent bare soil, growing season precipitation, and longest flow path length, as these variables can easily be derived for other burned hillslopes. These models were tested using data from other Colorado Front Range fires and had NSCE values ranging from 0.26–0.32 for all test fires combined, but varying performance for each individual fire. Although model performance declined for test fires, it still exceeded the performance of two more complex models applied at the same fires. The empirical models have the advantage of requiring limited input data, but they may not be valid for other regions and climates. Future applications should evaluate whether these types of simple parsimonious models are transferable to other geographic areas and evaluate the range of spatial scales at which the models can be applied.

Acknowledgements

We would like to thank the U.S. Forest Service and private land owners for facilitating access to our study sites and the many field assistants who helped gather data at High Park Fire, especially Stephen Small, Cassidi Rosenkrance, Emily Chavez, Hunter Gleason, and Adam Johnson. High Park Fire research was conducted under National Science Foundation grants DIB-1230205, DIB-1339928, and DGE-0966346. We also thank Juan Benavides-Solorio, Joe Wagenbrenner, Daniella Rough, Jay Pietraszek, Ben Snyder, and the many researchers who contributed to the collection of data from the test fires.

Appendix A. Supplementary data

Supplementary data to this article can be found online at https://doi.org/10.1016/j.catena.2017.12.029.

References

ARS (Agriculture Research Service), 2013. Rainfall intensity summarization tool (RIST) (version 3.89) [computer software]. Retrieved from United States Department of Agriculturehttp://www.ars.usda.gov/Research/docs.htm?docid=3251.
BAER (Burned Area Emergency Response), 2012. High Park Fire Burned Area Emergency Response (BAER) Report. High Park Fire Emergency Stabilization Plan, 12 July 2012.
Benavides-Solorio, J.D.D., MacDonald, L.H., 2001. Post-fire runoff and erosion from simulated rainfall on small plots, Colorado Front Range. Hydrol. Process. 15, 2931–2952. http://dx.doi.org/10.1002/hyp.383.
Benavides-Solorio, J.D.D., MacDonald, L.H., 2005. Measurement and prediction of post-fire erosion at the hillslope scale, Colorado Front Range. Int. J. Wildland Fire 14, 457–474. http://dx.doi.org/10.1071/WF05042.
Beven, K.J., Kirkby, M.J., 1979. A physically based, variable contributing area model of basin hydrology/Un modèle à base physique de zone d'appel variable de l'hydrologie du bassin versant. Hydrol. Sci. J. 24 (1), 43–69.
Brogan, D.J., Nelson, P.A., MacDonald, L.H., 2017. Reconstructing extreme post-wildfire floods: a comparison of convective and mesoscale events. Earth Surf. Process. Landf. 42 (15), 2505–2522. http://dx.doi.org/10.1002/esp.4194.
Brown, L.C., Foster, G.R., 1987. Storm erosivity using idealized intensity distributions. Trans. ASAE 30 (2), 379–386.
Canfield, H.E., Goodrich, D.C., 2005. Suggested Changes to AGWA to Account for Fire (V 2.1). USDA-ARS Southwest Watershed Research Center, Tucson, AZ.
Dennison, P.E., Brewer, S.C., Arnold, J.D., Moritz, M.A., 2014. Large wildfire trends in the western United States, 1984–2011. Geophys. Res. Lett. 41, 2928–2933. http://dx.doi.org/10.1002/2014GL059576.
Elliott, W.J., 2004. WEPP internet interfaces for forest erosion prediction. J. Am. Water Resour. Assoc. (April), 299–309.
Fernández, C., Vega, J.A., Vieira, D.C.S., 2010. Assessing soil erosion after fire and rehabilitation treatments in NW Spain: performance of RUSLE and revised Morgan–Morgan–Finney models. Land Degrad. Dev. 21 (1), 58–67.
Fernandez, C., Vega, J.A., Jimenez, E., Fonturbel, T., 2011. Effectiveness of three post-fire treatments at reducing soil erosion in Galicia (NW Spain). Int. J. Wildland Fire 20 (1), 104–114. http://dx.doi.org/10.1071/WF09010.
Flanagan, D.C., Livingston, S.J., 1995. WEPP user summary. NSERL Report No. 11. National Soil Erosion Research Laboratory, West Lafayette, IN.
Flannigan, M.D., Krawchuk, M.A., de Groot, W.J., Wotton, B.M., Gowman, L.M., 2009. Implications of changing climate for global wildland fire. Int. J. Wildland Fire 18, 483–507. http://dx.doi.org/10.1071/WF08187.
Gelman, A., Carlin, J.B., Stern, H.S., Rubin, D.B., 2004. Bayesian Data Analysis, 2nd ed. Chapman & Hall/CRC, New York, NY.
Goode, J.R., Luce, C.H., Buffington, J.M., 2012. Enhanced sediment delivery in a changing climate in semi-arid mountain basins: implications for water resource management and aquatic habitat in the northern Rocky Mountains. Geomorphology 139–140, 1–15. http://dx.doi.org/10.1016/j.geomorph.2011.06.021.
Goodrich, D.C., Canfield, H.E., Burns, I.S., Semmens, D.J., Miller, S.N., Hernandez, M., Levick, L.R., Guertin, D.P., Kepner, W.G., 2005. Rapid post-fire hydrologic watershed assessment using the AGWA GIS-based hydrologic modeling tool. Managing watersheds for human and natural impacts: engineering, ecological, and economic challenges. Am. Soc. Civil Eng. http://dx.doi.org/10.1061/9780784407639.
Hastings, B.E., Kampf, S.K., 2014. Evaluation of digital channel network derivation methods in a glaciated subalpine catchment. Earth Surf. Process. Landf. 39 (13), 1790–1802.
Huffman, E.L., MacDonald, L.H., Stednick, J.D., 2001. Strength and persistence of fire-induced soil hydrophobicity under ponderosa and lodgepole pine, Colorado Front Range. Hydrol. Process. 15, 2877–2892. http://dx.doi.org/10.1002/hyp.379.
Kampf, S.K., Brogan, D.J., Schmeer, S., MacDonald, L.H., Nelson, P.A., 2016. How do geomorphic effects of rainfall vary with storm type and spatial scale in a post-fire landscape? Geomorphology 273, 39–51.
Laflen, J.M., Elliot, W.J., Simanton, J.R., Holzhey, C.S., Kohl, K.D., 1991. WEPP: soil erodibility experiments for rangeland and cropland soils. J. Soil Water Conserv. 46 (1), 39–44.
Larsen, I.J., MacDonald, L.H., 2007. Predicting postfire sediment yields at the hillslope scale: testing RUSLE and disturbed WEPP. Water Resour. Res. 43 (11). http://dx.doi.org/10.1029/2006WR005560.
Larsen, I.J., MacDonald, L.H., Brown, E., Rough, D., Welsh, M., 2009. Causes of post-fire runoff and erosion: water repellency, cover, or soil sealing? Soil Sci. Soc. Am. J. 73, 1393–1407. http://dx.doi.org/10.2136/sssaj2007.0432.
MacDonald, L.H., Stednick, J.D., 2003. Forests and Water: A State-of-the-Art Review for Colorado. Colorado Water Resources Research Institute, Fort Collins, CO (Completion Report No. 196, 65. pp.).
Mayor, Á.G., Bautista, S., Bellot, J., 2011. Scale-dependent variation in runoff and sediment yield in a semiarid Mediterranean catchment. J. Hydrol. 397 (1), 128–135.
Miller, J.D., Safford, H.D., Crimmins, M., Thode, A.E., 2009. Quantitative evidence for increasing forest fire severity in the Sierra Nevada and Southern Cascade Mountains, California and Nevada, USA. Ecosystems 12, 16–32. http://dx.doi.org/10.1007/s10021-008-9201-9.
Miller, M.E., MacDonald, L.H., Robichaud, P.R., Elliot, W.J., 2011. Predicting post-fire hillslope erosion in forest lands of the western United States. Int. J. Wildland Fire 20 (8), 982–999. http://dx.doi.org/10.1071/WF09142.
Moody, J.A., Martin, D.A., 2009. Synthesis of sediment yields after wildland fire in different rainfall regimes in the western United States. Int. J. Wildland Fire 18, 96–115. http://dx.doi.org/10.1071/WF07162.
Moreland, D.C., 1980. Soil Survey of Larimer County Area, Colorado. USDA Soil Conservation Service and Forest Service, CO (181 pp.).
Morris, S.E., Moses, T.A., 1987. Forest fire and the natural soil erosion regime in the Colorado Front Range. Ann. Assoc. Am. Geogr. 77 (2), 245–254.
Natural Resource Conservation Service (NRCS), 2013. High Park Fire, Post-Fire Mulch Cover Specifications and Protocols. Fort Collins Field Office (Unpublished Report).
Nearing, M.A., 1998. Why soil erosion models over-predict small soil losses and under-predict large soil losses. Catena 32, 15–22.
Neary, D.G., Klopatek, C.C., DeBano, L.F., Ffolliott, P.F., 1999. Fire effects on below-ground sustainability: a review and synthesis. For. Ecol. Manag. 122, 51–71. http://dx.doi.org/10.1016/S0378-1127(99)00032-8.
Pietraszek, J.H., 2006. Controls on Post-fire Erosion at the Hillslope Scale, Colorado Front Range (Ph.D. thesis). Department of Forest, Rangeland, and Watershed Stewardship, Colorado State University, Fort Collins, CO.
Prats, S.A., Wagenbrenner, J.W., Martins, M.A.S., Malvar, M.C., Keizer, J.J., 2016. Mid-term and scaling effects of forest residue mulching on post-fire runoff and soil erosion. Sci. Total Environ. 573, 1242–1254.

PRISM Climate Group Oregon State University. http://prism.oregonstate.edu.
Renard, K.G., Foster, G.R., Weesies, G.A., McCool, D.K., Yoder, D.C., 1997. Predicting Soil Erosion by Water: A Guide to Conservation Planning With the Revised Universal Soil Loss Equation (RUSLE) (Agriculture handbook number 703). Agricultural Research Service, U.S. Department of Agriculture, Washington D.C.
Renard, K.G., Yoder, D.C., Lightle, D.T., Dabney, S.M., 2011. Universal soil loss equation and revised universal soil loss equation. In: Morgan, R.P.C., Nearing, M.A. (Eds.), Handbook of Erosion Modeling, 1st ed. Blackwell, pp. 137–167.
Rivix LLC, 2004. RiverTools 3.0. User's Guide. Rivix Limited Liability Company, Broomfield, CO (218 pp.).
Robichaud, P.R., Brown, R.E., 2002. Silt Fences: An Economical Technique for Measuring Hillslope Soil Erosion. USDA Forest Service, Fort Collins, CO (General Technical Report RMRS-GTR-94, 24 pp.).
Robichaud, P.R., Lillybridge, T.R., Wagenbrenner, J.W., 2006. Effects of postfire seeding and fertilizing on hillslope erosion in north-central Washington, USA. Catena 67, 56–67.
Robichaud, P.R., Elliot, W.J., Pierson, F.B., Hall, D.E., Moffet, C.A., 2007. Predicting postfire erosion and mitigation effectiveness with a web-based probabilistic erosion model. Catena 71, 229–241.
Robichaud, P.R., Lewis, S.A., Wagenbrenner, J.W., Ashmun, L.E., Brown, R.E., 2013a. Post-fire mulching for runoff and erosion mitigation, part I: effectiveness at reducing hillslope erosion rates. Catena 105, 75–92. http://dx.doi.org/10.1016/j.catena.2012.11.015.
Robichaud, P.R., Jordan, P., Lewis, S.A., Ashmun, L.E., Covert, S.A., Brown, R.E., 2013b. Evaluating the effectiveness of wood shred and agricultural straw mulches as a treatment to reduce post-wildfire hillslope erosion in southern British Colombia, Canada. Geomorphology 197, 21–33. http://dx.doi.org/10.1016/j.geomorph.2013.04.024.
Robichaud, P.R., Elliot, W.J., Lewis, S.A., Miller, M.E., 2016. Validation of a probabilistic post-fire erosion model. Int. J. Wildland Fire 25, 337–350.
Russo, D., Russo, I., Laufer, A., 1997. On the spatial variability of parameters of the unsaturated hydraulic conductivity. Water Resour. Res. 33 (5), 947–956.
Schaffrath, K., 2009. Changes in Erosion Rates and Ground Cover Over Time, Hayman and Schoonover Fires (M.S. Thesis). Colorado State University.
Schmeer, S.R., 2014. Post-fire Erosion Response and Recovery, High Park Fire, Colorado (M.S. Thesis). Colorado State University.
Shakesby, R.A., Doerr, S.H., 2006. Wildfire as a hydrological and geomorphological agent. Earth Sci. Rev. 74, 269–307. http://dx.doi.org/10.1016/j.earscirev.2005.10.006.
Spigel, K.M., Robichaud, P.R., 2007. First-year post-fire erosion rates in bitterroot National Forest, Montana. Hydrol. Process. 21, 998–1005. http://dx.doi.org/10.1002/hyp.6295.
Stone, B., 2015. Mapping Burn Severity, Pine Beetle Infestation, and Their Interactions at the High Park Fire (M.S. Thesis). Colorado State University.
Terranova, O., Antronico, L., Coscarelli, R., Iaquinta, P., 2009. Soil erosion risk scenarios in the Mediterranean environment using RUSLE and GIS: an application model for Calabria (southern Italy). Geomorphology 112 (3), 228–245.
Thompson, J.A., Bell, J.C., Butler, C.A., 2001. Digital elevation model resolution: effects on terrain attribute calculation and quantitative soil-landscape modeling. Geoderma 100 (1), 67–89.
USDA Natural Resources Conservation Service, 1998. Official soil series description. Available at. https://soilseries.sc.egov.usda.gov/OSD_Docs/R/REDFEATHER.html, Accessed date: 30 December 2016.
Vafeidis, A.T., Drake, N.A., Wainwright, J., 2007. A proposed method for modelling the hydrologic response of catchments to burning with the use of remote sensing and GIS. Catena 70 (3), 396–409.
Van Eck, C.M., Nunes, J.P., Vieira, D.C.S., Keesstra, S., Keizer, J.J., 2016. Physically-based modeling of the post-fire runoff response of a forest catchment in central Portugal: using field versus remote sensing based estimates of vegetation recovery. Land Degrad. Dev. 27, 1535–1544.
Wagenbrenner, J.W., Robichaud, P.R., 2014. Post-fire bedload sediment delivery across spatial scales in the interior western United States. Earth Surf. Process. Landf. 39, 865–876. http://dx.doi.org/10.1002/esp.3488.
Wagenbrenner, J.W., MacDonald, L.H., Rough, D., 2006. Effectiveness of three post-fire rehabilitation treatments in the Colorado Front Range. Hydrol. Process. 20, 2989–3006. http://dx.doi.org/10.1002/hyp.6146.
Wagenbrenner, J.W., MacDonald, L.H., Coats, R.N., Robichaud, P.R., Brown, R.E., 2015. Effects of post-fire salvage logging and a skid trail treatment on ground cover, soils, and sediment production in the interior western United States. For. Ecol. Manag. 335, 176–193. http://dx.doi.org/10.1016/j.foreco.2014.09.016.
Wischmeier, W.H., Smith, D.D., 1978. Predicting Rainfall Erosion Losses – A Guide to Conservation Planning. U.S. Department of Agriculture (Handbook No. 537).
Woolhiser, D.A., Smith, R.E., Goodrich, D.C., 1990. KINEROS, A Kinematic Runoff and Erosion Model: Documentation and User Manual. U.S. Department of Agriculture, Agricultural Research Service (ARS-77, 130 pp.).